Evaluation of Spacecraft Modal Test Methods

Jay-Chung Chen*
Jet Propulsion Laboratory, California Institute of Technology, Pasadena, California

Modal testing methods have undergone great changes in recent years as new testing methods are being created. Although devoted advocates of each method can be found to argue the relative advantages and disadvantages, the general superiority, if any, of one or the other is not yet evident. The present paper evaluates various modal testing methods based on the results of tests performed on a complex, realistic spacecraft structural system. It concludes that the selection of a modal testing method should be determined by the test requirement, constraints, and nature of the test article.

Nomenclature

$[M]$ = mass matrix
$[C]$ = damping matrix
$\{F(t)\}$ = external excitation vector
$[K]$ = stiffness matrix
$\{\ddot{x}\}$ = acceleration response vector
$\{\dot{x}\}$ = velocity response vector
$\{x\}$ = displacement response vector
α, β = scalar coefficients
$[\gamma_n]$ = percentage of critical damping
$[\omega_n^2]$ = eigenvalues
$[\phi]$ = normal mode matrix
$[I]$ = identity matrix
$\{q\}$ = generalized coordinates defined by Eq. (5)
$\{g_\eta\}$ = generalized external forces
$\{f\}$, = shaker force vector
a_i, b_i = coefficients
Ω = shaker frequency
s = Laplace variable
$(\text{frf})_{ij}$ = element of ij of the frequency response function matrix

Introduction

MODAL testing plays a significant role in spacecraft development where the experimentally determined nature frequencies, mode shapes, and other modal parameters are used to verify the analytical model for design. Although the traditional modal test method was first proposed in 1950,[1] this so-called "multishaker sine dwell" method is still used extensively in the aerospace industry. However, with the advent of microcomputers and minicomputers, "frequency response function" methods become popular.[2] Some detailed comparisons of these two approaches would have been beneficial. But so far most of the comparisons have been made on relatively simple structures such as beams or plates. Only limited actual testing comparisons have been performed on realistic complex structures.[3,4] In the summer of 1983, the Galileo spacecraft modal test provided an opportunity to evaluate these modal testing methods. The results of the evaluation are the subject of the present report.

Received April 4, 1984; presented as Paper 84-1069 at the AIAA Dynamics Specialist Conference, Palm Springs, CA, May 17–18, 1984; revision received March 16, 1986.

*Member Technical Staff, Applied Technologies Section. Member AIAA.

Basically all modal testing can be viewed as a forced vibration test in which external forces are applied and responses are measured. The multishaker sine dwell method concentrates the shaker frequency at a certain discrete value and appropriates certain shaker force distribution. The objective is to make the responses similar to a specific mode shape. The eigenvalues and eigenvectors, i.e., the natural frequencies and the mode shapes, respectively, are measured directly and no further data processing is necessary. Also, since the structure is responding in steady state, no high speed data acquisition and analysis capability is required once the mode is tuned. On the other hand, the frequency response function methods make sure that excitation inputs contain all the frequencies such that all the modes of interest are excited simultaneously. Modal parameters such as the natural frequencies, mode shapes, and dampings are extracted from the response data. Therefore, it is necessary that high speed data acquisition and analysis systems are available to process the data. It became clear why the multishaker sine dwell method was the only modal testing technique more than thirty years ago and the frequency response function methods were not possible until microprocessor technology matured. (A detailed description of the development of testing methods and an extensive bibliography can be found in Ref. 5.)

These drastically different testing methods each have their own advantages and disadvantages and, as such, have their own ardent devotees. The objective of the present study is not to evaluate the ease or difficulty in implementing these testing techniques since the experiences, the test engineer, and the complexity of the test article are the foremost factors in determining the quality of the test results. Therefore, the present evaluation will be focused on two aspects of the modal test. One is the theory on which the testing method is based. The inherent difficulties of satisfying theoretical assumptions will be examined for the different testing techniques.

The second aspect is to evaluate the results of the modal testing of the same test article in terms of the quality of the results. Although an identical test article and instrumentation were used in the applications of these different testing methods, different test personnel were in charge of implementing the different methods. Since each of them has been involved in the development of their chosen modal testing method and has extensive experience in using the particular method, the quality of test personnel should be assured.

Theoretical Background

In the evaluation of modal testing methods, the differences in the theoretical approach are obviously of prime concern. As mentioned before, the following brief theoretical description is for the purpose of examining the inherent constraints of the modal testing methods.

The equations of motion for an n-DOF (degrees-of-freedom) linear damped system under external excitation can be written as

$$[M]\{\ddot{x}\}+[C]\{\dot{x}\}+[K]\{x\}=\{F(t)\} \quad (1)$$

where $[M]$, $[C]$, and $[K]$ are the mass, damping, and stiffness matrices of the structure, respectively, and $\{F(t)\}$ is the external forcing function vector. The system represented by Eq. (1) is said to possess classical normal modes if and only if it can be reduced to a set of uncoupled second order systems. A necessary and sufficient condition for the existence of classical normal modes is that matrices $[M]^{-1}[C]$ and $[M]^{-1}[K]$ commute[6]

$$[M]^{-1}[C][M]^{-1}[K]=[M]^{-1}[K][M]^{-1}[C] \quad (2)$$

However, the dampings provided by the spacecraft structural system are usually small. For analytical simplicity, it is often assumed that the dampings are proportional to mass and stiffness

$$[C]=\alpha[M]+\beta[K] \quad (3)$$

where α and β are arbitrary proportional constants. The existence of the classical normal modes assures the following orthogonality conditions:

$$\left.\begin{aligned}[\phi]^T[M][\phi]&=[\,I\,]=\text{Unity matrix}\\ [\phi]^T[C][\phi]&=[\,2\gamma_n\omega_n\,]\\ [\phi]^T[K][\phi]&=[\,\omega^2\,]\end{aligned}\right\} \quad (4)$$

where $[\phi]$ is the normal mode or eigenvector matrix, $[\,\gamma_n\,]$ is the percentage of critical damping, and $[\,\omega_n^2\,]$ is the eigenvalues. Now, applying the modal transformation

$$\{x\}=[\phi]\{q\} \quad (5)$$

the governing equation, Eq. (1), can be written as

$$\{\ddot{q}\}+[\,2\gamma_n\omega_n\,]\{\dot{q}\}+[\,\omega^2\,]\{q\}=[\phi]^T\{F(t)\} \quad (6)$$

Once the external forces $\{F(t)\}$ are defined, the motion of the system may be obtained by Eqs. (5) and (6).

Table 1 TAM prediction

Mode no.	Frequency, Hz	Description
1	11.08	SXA in Y
2	11.20	SXA in X
3	14.94	Global bending in X
4	15.08	Global bending in Y
5	16.36	1st global torsion
6	20.04	RTG walking mode
7	20.37	Appendages in Z
8	21.03	2nd global torsion
9	23.53	Science boom in Z
10	24.87	Sun shade in Z
11	25.33	Probe in Y
12	26.41	EDP in Y
13	30.67	Thruster booms in Y, out of phase
14	31.77	Thruster booms in Y, in phase
15	32.21	RRH in Y
16	32.78	Global bounce mode Z
17	33.03	RRH in Y
18	34.81	400 N. engine in Y
19	35.35	Science boom in X-Y
20	35.51	400 N. engine in Y

Multishaker Sine Dwell Method

For the case of the multishaker sine dwell method, the external forces are sinusoidal with frequency Ω, therefore,

$$\{F(t)\}=\{f\}\sin\Omega t \quad (7)$$

where $\{f\}$ represents the amplitudes of the forces distributed on the system and Ω is the frequency of these forces. The generalized forces in Eq. (6) will be defined as

$$[\phi]^T\{F(t)\}=[\phi]^T\{f\}\sin\Omega t=\{g_n\}\sin\Omega t \quad (8)$$

The acceleration responses can be obtained from Eqs. (5) and (6) as

$$\{\ddot{x}\}=\left(\sum_{i=1}^{i=n}a_i g_i\{\phi_i\}\right)\sin\Omega t+\left(\sum_{i=1}^{i=n}b_i g_i\{\phi_i\}\right)\cos\Omega t \quad (9)$$

where

$$\left.\begin{aligned}a_i&=\frac{-\left[1-\left(\frac{\Omega}{\omega_i}\right)^2\right]}{\left[1-\left(\frac{\Omega}{\omega_i}\right)^2\right]^2+4\gamma_i^2\left(\frac{\Omega}{\omega_i}\right)^2}\\ b_i&=\frac{2\gamma_i\left(\frac{\Omega}{\omega_i}\right)}{\left[1-\left(\frac{\Omega}{\omega_i}\right)^2\right]^2+4\gamma_i^2\left(\frac{\Omega}{\omega_i}\right)^2}\\ g_i&=\{\phi_i\}^T\{f\}\\ \{\phi_i\}&=i\text{th normal mode, a subset of }[\phi]\end{aligned}\right\} \quad (10)$$

The first and second parts of the right-hand side of Eq. (9) are also known as CO (coincidence) and QUAD (quadrature) responses because of their in-phase and 90 deg out-of-phase nature with respect to the input forces.

According to Lewis and Wrisley,[1] a number of shakers could be "tuned" to "exactly" balance the dissipative forces in a structure at a certain frequency. The external forces will be assumed as

$$\{f\}=[C]\{\dot{x}\} \quad (11)$$

and the response of the structure will be, for example, the jth mode. Hence,

$$\{x\}=\{\phi_j\} \quad (12)$$

The shaker forces will become, according to Eq. (11),

$$\{f\}=[C]\{\phi_j\} \quad (13)$$

When substituting Eq. (13) into the generalized forces in Eq. (9) and using Eqs. (3) and (4), one obtains

$$\left.\begin{aligned}g_i&=0 \quad \text{for } i\neq j\\ g_j&\neq 0 \quad \text{for } i=j\end{aligned}\right\} \quad (14)$$

Next, the forcing function frequency will be "tuned" to that of the jth resonance frequency, i.e.,

$$\Omega=\omega_j \quad (15)$$

The a_i's and b_i's can be obtained as

$$\left.\begin{aligned} a_i &= \frac{-\left[1-\left(\frac{\omega_j}{\omega_i}\right)^2\right]}{\left[1-\left(\frac{\omega_j}{\omega_i}\right)^2\right]^2+4\gamma_i^2\left(\frac{\omega_j}{\omega_i}\right)^2} \\ b_i &= \frac{2\gamma_i\left(\frac{\omega_j}{\omega_i}\right)}{\left[1-\left(\frac{\omega_j}{\omega_i}\right)^2\right]^2+4\gamma_i^2\left(\frac{\omega_j}{\omega_i}\right)^2} \end{aligned}\right\} \quad \text{for } i\neq j,\ \omega_i\neq\omega_j$$

$$a_j=0, \qquad b_j=\frac{1}{2\gamma_j} \qquad \text{for } i=j \tag{16}$$

The acceleration responses, Eq. (9), become

$$\{\ddot{x}\}=\frac{1}{2\gamma_j}g_j\{\phi_j\}\cos\Omega t \tag{17}$$

Under this perfect condition, the response will be 90 deg out-of-phase from the input forces and its spatial distribution will be exactly that of the jth mode.

However, in practice, things are far from ideal. Only a very limited number of shakers will be available because of physical constraints, therefore, Eq. (11) cannot be satisfied. In other words, it is impossible to balance out the dissipative forces since one cannot install shakers at all the DOF's. Also, the jth mode shape cannot be known as an a priori condition: only an estimated one based on pretest analysis or engineering judgment is available. Therefore, Eq. (12) also is not satisfied. At best, the force distribution as expressed in Eq. (13) is an approximation

$$\{f\}\cong[C]\{\phi_j\} \tag{18}$$

and, according to Eq. (10),

$$g_i\neq 0 \qquad \text{for } i=1,2,3,\ldots n$$

but

$$g_j\gg g_i \text{ for } i\neq j \tag{19}$$

Compared to the shaker force appropriation, the frequency is easier to "tune" to one of the resonance frequencies during the test since both the 90 deg out-of-phase and maximum amplitude criteria can be used. The resonance condition in Eq. (15) or a very close one can be achieved. Therefore, Eq. (16) implies that for an "almost tuned" jth mode, the following are valid:

$$\left.\begin{aligned} b_j &\gg b_i \qquad \text{for } i\neq j \\ |a_i| &< 1.0 \qquad \text{for all } i \end{aligned}\right\} \tag{20}$$

With these considerations, the acceleration response, Eq. (10), will be

$$\{\ddot{x}\}=b_jg_j\{\phi_j\}\cos\Omega t+\text{contamination} \tag{21}$$

where contamination is:

$$\sum_{i=1}^{i=n}\left[(a_ig_i\sin\Omega t+b_ig_i\cos\Omega t)\{\phi_i\}\right] \quad \text{for } i\neq j \tag{22}$$

Based on Eqs. (19) and (20), the first term of the right-hand side of Eq. (21) is much greater than the contamination terms. This indicates that the response measurements are indeed very close to the jth mode.

For the case of very close modal frequencies, or similar mode shapes, the inequalities in Eqs. (19) and (20) are weakened. This increases the amplitude of contamination and decreases the accuracy of the mode shape measurements. To overcome the deficiency, the shaker force appropriation must be improved. It is evident that the key issue of the multishaker sine dwell is the shaker force appropriation that has generated many studies.[7-10] However, none has been accepted as an industry standard.

In summary, the inherent constraints of the multishaker sine dwell method are the inability to tune the "pure" mode except in very limited cases and the difficulty in separating the close modes.

Frequency Response Function Method

In the form of Laplace transformation, the solution of Eq. (1) can be written as

$$\{x(s)\}=[\phi]\left[\left(s^2+2\gamma_n\omega_ns+\omega_n^2\right)\right]^{-1}[\phi]^T\{F(s)\} \tag{23}$$

where $x(s)$ and $F(s)$ are the Laplace transforms of $x(t)$ and $F(t)$, respectively. Furthermore, if one substitutes the Laplace variable s by $i\Omega$, the acceleration responses of the system can be obtained

$$\{x(i\Omega)\}=[\phi]\left[\left(a_i+ib_i\right)\right][\phi]^T\{F(i\Omega)\} \tag{24}$$

where a_i and b_i are defined in Eq. (10) and the frequency response function (frf) is defined as

$$[(\text{frf})_{ij}]=[\phi]\left[\left(a_i+ib_i\right)\right][\phi]^T \tag{25}$$

Eq. (25) contains all the information related to the modal parameters, namely, mode shapes, frequencies, and damping. The concept of the frequency response function modal test method is to develop a curve-fitting procedure for Eq. (25) that determines all the modal parameters.

If a single shaker is used during the test, the element in one column of the $[(\text{frf})_{ij}]$ matrix can be readily obtained by dividing the measured responses by the input forces—the concept of transfer function. It can be shown that only a single column of a single row of the $[(\text{frf})_{ij}]$ matrix is needed for determining all the modal parameters, if no repeated roots are involved.

If multiple shakers are used, in principle, multiple rows or columns of the frequency response function matrix can be obtained. There are algorithms that utilize as much of the redundant information within these frequency response functions as possible. A primary example is the Poly Reference approach.[11]

The brief description previously given for the frequency response function method of modal testing indicated that the approach is based on sound theory and seemingly no constraint is apparent in its modal parameter extraction concept. Although one may question the accuracy of the curve-fitting procedure, the concept is valid, nevertheless. However, one of the most important aspects of this approach has yet to be discussed. This concerns how the measured time domain data are transformed into the frequency domain data for the modal parameter extraction process. The Fourier transform serves as the bridge between the time and frequency domain functions. The basis is a Fourier transform pair for continuous signals defined as follows:

$$\begin{aligned} X(f) &= \int_{-\infty}^{\infty} x(t)\,e^{-i2\pi ft}\,dt \\ x(t) &= \int_{-\infty}^{\infty} X(f)\,e^{i2\pi ft}\,df \end{aligned} \tag{26}$$

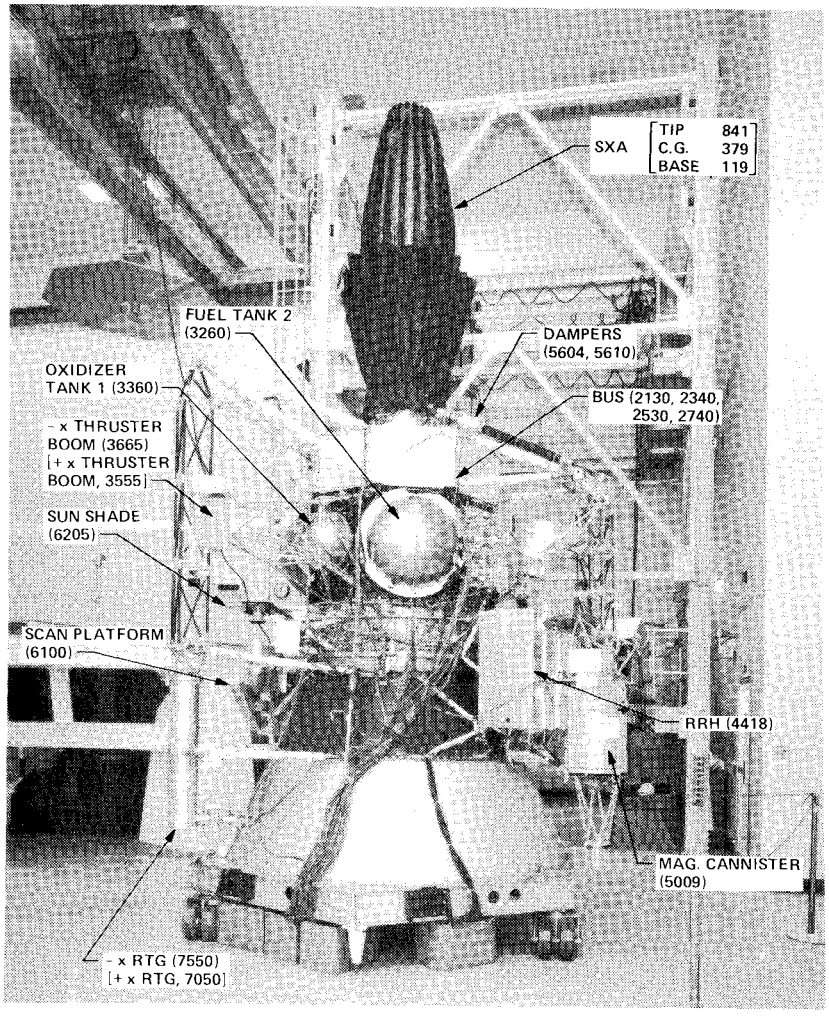

Fig. 1 Galileo spacecraft in modal test configuration.

The upper-case $X(f)$ represents the frequency domain functions, and the lower-case $x(t)$ is the time domain function. Their relationship is governed by Eq. (26). However, when the measured time domain data are sampled and analyzed, it is the finite, discrete version of the Fourier transform, or the Fourier series expansion, that must be used. The analogous discrete Fourier transform pair is as follows:

$$X(\omega_j) = \frac{1}{N}\sum_{k=0}^{N-1} x(t_k)\, e^{-i2\pi j\frac{k}{N}}$$

$$x(t_k) = \sum_{j=0}^{N-1} X(\omega_j)\, e^{i2\pi j\frac{k}{N}}$$

$$j = 0,1,2,\ldots,N-1; \qquad k = 0,1,2,\ldots,N-1 \quad (27)$$

Although most of the properties of the continuous Fourier transform are retained, several differences result from the constraint that the discrete Fourier transform places on time domain data defined over finite intervals. The so-called "Cooley-Tukey fast Fourier transform" (FFT) algorithm is an efficient method for computing the discrete Fourier transform. The FFT can be used in place of the continuous Fourier transform only to the extent that the discrete Fourier transform could be used before, but with a substantial reduction in computer time. Some of the inherent constraints of the discrete Fourier transform are briefly described.

The sampling theorem states that if the Fourier transform of a continuous function is zero for all frequencies greater than a certain frequency f_c, then the said continuous function can be uniquely determined from a knowledge of its discrete function with a sampling rate of $2f_c$, which is referred to as the Nyquist sampling rate.[12] In practice, when the sampling rate is not sufficiently high for the time domain function measurement, its Fourier transform will be distorted by the high frequency component. This is also known as "aliasing." Usually a low pass filter is used to eliminate the high frequency component.

Another problem is the "leakage" that is inherent in the Fourier analysis of any finite record of data. The effect of truncation at other than a multiple of the period creates a periodic function with sharp discontinuities. The result is a series of spurious peaks that appear because of this abrupt ending of the signal in time domain. These "leakages" in the frequency domain seriously affect the accuracy of the curve-fitting procedure. The usual approach to reduce the leakage is to apply a data window to the time domain function, which has lower spurious peaks in the frequency domain than those of the rectangular data windows. One of the most commonly used data windows is the Hanning window.

In summary, the inherent constraints of the frequency response function modal test method are the leakage and aliasing problems. However, the effects of these problems can be reduced by applying anti-aliasing filters, increasing the sampling rate, and choosing proper time domain functions and windows.

Galileo Spacecraft Modal Test

The Galileo is an interplanetary spacecraft whose mission is to conduct a scientific exploration of the planet Jupiter. It will

be launched by the Space Shuttle and a modified Centaur Upper Stage in 1987. Figure 1 shows the Galileo spacecraft in its modal test configuration with its major components and corresponding finite-element node numbers indicated. The total weight of the spacecraft is approximately 5300 lb. A finite-element model using the NASTRAN code was constructed for performing the design loads analysis. This model consists of approximately 10,000 static DOF and 1600 dynamic DOF. It is this loads analysis model which has to be verified by the modal test.

Extensive pretest analysis was conducted prior to the modal test[13] for the purpose of understanding the modal characteristics of the loads model. This was essential in the design of the modal test, including the instrumentation distribution and external excitation selection. After careful consideration, it was determined that 162 channels of accelerometer measurements, as well as 118 channels of strain gage measurements, were to be taken. The instrumentation distribution was such that all the important modal displacements and modal forces were measured with sufficient resolution. Since the number of DOF's in the loads analysis model was a few orders of magnitude greater than the number of measurements to be made during the test, a condensed model was constructed so that this DOF would be compatible with the measurements. This condensed model was called the Test-Analysis Model (TAM), which was obtained by Guyan reduction method[14] to collapse the mass and stiffness matrices in the loads analysis model onto 162 DOF. The TAM was adjusted so that all the modal characteristics predicted by the loads model would be reproduced by TAM within the range of interest. Table 1 shows the TAM prediction of the modes.

The modal test was performed with various testing methods and their detailed descriptions and results can be found in Refs. 15–18. Table 2 summarizes the methods used and the participants associated with these methods. These participants have all been involved in modal testing for a number of years, especially using their chosen methods. Their professional dedication assures high quality test results. Figure 2 shows typical response functions for various methods.

Results Comparisons

Table 3 lists the frequencies of the normal modes obtained by the methods listed in Table 2, with the exception of Tuned Sweep. (Incomplete channels of data were taken for the Tuned Sweep method.) The correlation of the modes obtained by the various methods is carried out by examining not only the frequencies but also the mode shapes, cross-orthogonality between modes from different methods, effective mass, and kinetic energy distribution. It was pointed out in the pretest analysis (Ref. 13) that vibration modes are not equal in degrees of importance with respect to the loads analysis in the design process. Some modes contribute to the dynamic loads more heavily than others and these important modes are usually the target modes to be verified in a modal test. The important modes for the Galileo spacecraft loads analysis have been identified as global modes and all of them have been test verified by all the methods as shown in Table 3. Specifically, the effective mass and modal accelerations due to interface loadings are used to define the global modes as shown in Tables 4 and 5 and Ref. 13. Furthermore, the frequencies of these modes are consistent regardless of the method used. The two exceptions are that the first mode obtained by the 4-shaker random method is noticeably lower than the rest and the single point random method failed to obtain the fifth mode. As for the rest of the nonglobal modes (local modes), the following observations can be made:

1) Except for mode 30, in general the frequencies are in good agreement for all modes.

2) Mode 15, an analytical predicted local mode, is measured by the 3-shaker random method only. The 4-shaker random method as well as all others failed to obtain this mode.

3) Modes 16, 17, 20, 22, and 33, all predicted by the analysis, are measured by only some of the methods.

4) Modes 28, 30, 31, 32, and 33, all predicted by the analysis, are measured by only the frequency response function methods.

5) Modes 6, 7, 8, 23, 24, 25, and 26 are measured by only the single-shaker methods. Neither the multishaker random methods nor the analysis succeeded in identifying them.

6) In general, the frequency response function methods identified more modes than the sine dwell method.

7) Among the modes identified by the Simultaneous Frequency Domain method, several are suspicious.

The results of the sine dwell method and the 4-shaker random method will be chosen for more detailed comparison. First, the 4-shaker random method obtained 27 modes as compared to 14 modes by the sine dwell method. The global

Table 2 Summary of Galileo spacecraft modal test methods

No.	Methods	No. of shakers	Input function	Participant/organ.	Remark
1	Sine dwell	Up to 8	Sine	Trubert/JPL[a]	Required by Galileo project
2	Multishaker random	3	Random	Hunt/SDRC[b]	Uncorrelated signals for the shakers
3	Multishaker random	4	Random	Hunt/SDRC	Uncorrelated signals for the shakers
4	Single-point random	1	Random	Stroud/STI[c]	
5	CHIRP	1	Fast sine sweep	Stroud/STI	
6	SWIFT	1	Discrete sine sweep	Stroud/STI	frfs are obtained between the frequency changes
7	Tuned sweep	1	Discrete sine sweep	Stroud/STI	Sweep within narrow frequency band
8	SFD[d]	1	Random	Coppolino/MSC,[e] Stroud/STI	Used same frfs as no. 4
9	ERA[f]	1	Random decay	Pappa/LaRC[g] Stroud/STI	New modal parameter extraction algorithm

[a]Jet Propulsion Laboratory. [b]Structural Dynamics Research Corporation. [c]Synergistic Technology Incorporated. [d]Simultaneous Frequency Domain (Ref. 19). [e]MacNeal-Schwendler Corporation. [f]Eigensystem Realization Algorithm. [g]NASA Langley Research Center.

Table 3 Frequency comparison for various test methods

No.	TAM	Sine dwell	4-shaker random	3-shaker random	SWIFT	CHIRP	Single-pt. random	SFD	ERA	Description
1	11.08[a]	12.70	11.46	13.73	12.54	12.59	12.66	12.52	13.61	SXA in Y
2	11.20[a]	13.11	14.02	14.10	13.78	13.86	13.88	13.76	14.15	SXA in X
3	14.94[a]	17.41	18.54	18.62	17.40	17.95	18.14	17.47	18.37	Global bending in X
4	15.08[a]	17.76	17.44	18.32	17.62	17.97	17.93	17.62	18.68	Global bending in Y
5	16.36[a]	18.59	19.33	19.45	18.93	19.30	—	18.93	19.52	1st global torsion
6	—	—	—	—	18.22	18.54	18.54	18.37	—	SXA and $+X$ thruster in Y
7	—	—	—	—	18.59	18.59	18.62	18.74	—	SXA in X
8	—	—	—	—	19.31	19.34	19.31	19.45	—	RRH in Y
9	—	—	22.22	—	22.04	21.98	22.08	22.03	22.13	RTG in Z
10	20.04[a]	21.67	22.06	22.19	22.23	22.24	22.21	22.27	22.64	RTG walking mode
11	20.37	23.10	22.52	22.81	22.35	22.62	22.48	22.52	22.58	Appendages in Z
12	21.03[a]	25.46	25.80	25.80	25.30	25.71	25.74	25.37	—	2nd global torsion
13	23.53[a]	23.66	25.19	25.33	27.61	—	27.63	27.62	—	Science boom in Z
14	—	—	—	—	—	—	—	24.57	—	
15	24.87	—	—	28.16	—	—	—	—	—	Sun shade in Z
16	25.33	—	26.36	26.64	—	—	—	—	—	Probe in Y
17	26.41	—	—	—	26.83	25.75	—	26.86	26.65	EDP in Y
18	—	—	—	—	—	—	—	27.08	—	
19	—	—	—	—	—	—	—	28.81	—	
20	30.67	29.71	33.42	33.46	—	—	—	—	—	Thruster boom in YO/P
21	—	26.12	30.50	—	28.37	28.56	28.51	28.13	—	Damper in Y
22	31.77	42.20	39.14	—	—	—	—	—	—	Thruster boom in YI/P
23	—	—	31.84	31.92	29.48	—	—	29.47	—	Damper in X
24	—	—	—	—	33.02	33.21	33.13	33.04	33.29	Probe in X
25	—	—	—	—	33.63	33.74	33.64	33.69	33.61	Probe and + thruster in X
26	—	—	—	—	33.98	—	—	33.99	—	Mag. can. and DDS in X
27	—	—	33.76	—	33.40	33.80	—	33.35	—	Thruster in X
28	32.21	—	27.84	27.89	26.22	25.53	—	26.23	—	RRH in Y
29	32.78[a]	37.92	37.91	37.98	38.17	38.09	37.94	38.14	38.42	Global Z mode
30	33.03	—	28.29	28.58	39.70	—	—	39.75	39.55	RRH in Y
31	34.81	—	42.35	42.57	—	—	—	—	—	400 N. engine in Y
32	35.35	—	34.50	34.32	33.75	33.85	33.79	33.76	34.40	Science boom in X-Z
33	35.51	—	41.73	—	—	—	—	—	—	400 N. engine in Y
34	—	—	—	—	—	—	—	37.05	—	
35	—	—	39.77	—	—	—	—	—	—	Science boom in Y
36	—	—	—	39.88	41.01	—	—	41.11	—	RRH and mag. can. in Y
37	—	—	—	—	—	—	—	41.63	—	
38	—	—	—	—	—	—	—	42.04	—	
39	—	—	42.36	—	—	—	—	—	—	Thruster in Y
40	—	—	44.61	—	—	—	—	—	—	Thrusters in YI/P
41	—	42.53	44.98	45.14	42.99	—	—	42.98	44.27	Scan platform in X
42	—	—	46.00	46.05	44.82	44.70	44.34	44.86	44.89	Thrusters and RRH in Y
43	—	—	—	—	—	—	—	44.93	—	
No. of modes		14	27	21	27	21	18	34	16	

[a] Global mode.

Table 4 Effective mass for sine dwell modes

Mode	Frequency	x	y	z	θ_x	θ_y	θ_z
201	12.70	0.3	8.7	0	23.1	0.8	0
101	13.11	13.3	0.3	0	0.6	28.4	0
501	17.76	9.6	26.5	0.1	31.5	9.3	0.2
404	17.40	13.8	19.1	0	25.2	15.5	0.4
301	18.60	0	0	0	0	1.6	20.2
601	21.67	42.4	0.3	0.1	0.3	33.6	2.4
2050[a]	23.10	0	2.6	4	1.2	0.3	0.1
702[a]	23.66	0	0.6	6.7	1.1	0	0
803	25.16	0.8	0	0.2	0	0.3	23.2
902[a]	26.12	0.1	0.1	5.7	0.2	0	4.3
2902[a]	29.71	1	0.8	0	0.1	0.1	6.5
1503	37.92	0.2	0.2	45.8	0	0.2	0.1
2002[a]	42.20	0.1	0	0.4	0	0	0
1801[a]	42.53	0	0	1.2	0	0	0.1
		81.6	59.3	64.1	83.3	90.1	57.5

[a] Local modes.

modes, which are identified by their large components of the effective mass, are similar for both methods, as shown in Tables 4 and 5. The total effective mass is considered as a criterion for the completeness of the test. The comparison indicates that that total effective mass for the 4-shaker random results is 10–20% higher than that of the sine dwell method, with only half of the modes tested. This demonstrates that the sine dwell method is able to extract most of the important global modes with fewer modes tested. Tables 6 and 7 show the orthogonality of the modes obtained by the sine dwell and 4-shaker random methods, respectively. Off-diagonal terms greater than 0.10 are boxed, and the results show clearly that modes from the 4-shaker random test are much more orthogonal than those from the sine dwell test. In fact, if only the global modes are considered, the orthogonality of the sine dwell modes is not very good at all. Of course the errors could also be due to incorrect mass matrix used in the orthogonality check. The cross-orthogonality between the modes obtained by the two methods is shown in Table 8. The purpose of the table is to demonstrate the similarity of the mode shapes from these two methods. Ideally, if the modes are identical, the cross-orthogonality will be unity, 1,

for the same modes and zero for rest of the modes. In other words, there should be one value of 1 in each row and the rest of the numbers should be zero. Any deviation is an indication of discrepancies with respect to the orthogonality characteristics of the modes. For instance, mode 1 from the 4-shaker random test is correlated perfectly with mode 201 from the sine dwell test, and the rest of the modes from the 4-shaker random test are almost orthogonal with mode 201, as indicated by the numbers in the first row of Table 8. The overall indication of Table 8 is that some modes are very well correlated, especially the global modes, while others are not. For instance, mode 2050 from the sine dwell method is simultaneously correlated with 4-shaker modes 6, 7, 8, and 10.

Table 9 shows the mode shape comparison for the first mode. The modal amplitude is listed in the order of amplitude according to the TAM, with the maximum normalized to unity. The numbers in parentheses represent the sequential order of the modal amplitudes. It is obvious that the first mode is the antenna bending in the y direction since its larger motion is in that direction. The RSS 1 is the square root of the sum of the difference of TAM and test modal amplitude squared, and the RSS 2 is the similar value between the two test-obtained modes. It is interesting to note that differences between the TAM and test modes are much greater than the differences between the two test modes. Table 10 shows the mode shape comparison of the Radioisotope Thermal-electric Generator (RTG) walking modes. The predicted TAM value indicates that the two RTG's are moving symmetrically, although in opposite directions. However, both test modes indicate that one RTG amplitude is much higher than the other. Tables 11 and 12 show the kinetic energy distribution for the corresponding modes shown in Tables 9 and 10, respectively. For the first mode, more than 90% of the kinetic energy is in the y direction and more than 70% is concentrated at the SXA antenna. This mode is described as the SXA antenna bending in y direction. From Table 12 the kinetic energy for the RTG walking mode indicates that contrary to the TAM results, the energies of the two RTG's are indeed different. Careful examination of the test article showed physical difference in mass mockups. The kinetic energy distribution is a very useful tool in understanding the details of the modal characteristics.

Finally, the test-measured damping values are plotted in Figure 3. They are totally uncorrelated with the frequency.

Overview of Test Results

It must be emphasized here that conclusions from the present experiences are valid for the specific type of structural system that we tested, namely, the large, complex spacecraft. The basic objective for the modal test is to verify the analytical model for the design process. It tends to involve a large number of measurements and extensive test/analysis correlation. Of course it is recognized that there are many other

Table 5 Effective mass for multishaker random modes

Mode	Frequency	x	y	z	θ_x	θ_y	θ_z
1	11.46	0.7	4.8	0	14.8	1.5	0
2	14.02	22.7	0.2	0.4	0.7	48	0
3	17.44	1.8	41.6	0.3	52.1	1.7	0
4	18.54	18.6	0.5	0.2	0.6	17.2	4.7
5	19.33	0	0.2	0	0.1	0.6	19.4
6	22.06	21.3	2.9	0.3	1.3	14.2	1.3
7	22.52	3.6	14.8	1.5	5.4	1.5	0.9
8	25.19	0	1.7	12.5	0.1	0	1.6
9	25.80	1.3	0.8	1.9	0.8	0.6	22
10[a]	26.36	0	3.3	0	0.4	0	0.3
11[a]	27.84	0.1	0.1	3.8	0	0.1	1.7
12[a]	28.29	0.3	0.4	0	0.1	0	0.7
13[a]	30.50	0.7	0	5.7	0.9	0.9	0
14[a]	31.84	0.2	0.5	0.1	0.2	0.1	7.1
15	33.42	13.3	0	0.9	0.1	3.8	0.2
16[a]	33.76	3.8	0.7	0.1	0.1	1.2	4.6
17[a]	34.50	0.8	0.2	0	0	0.2	2.2
18	37.91	0.1	0.2	45.6	0.1	0.1	0
19[a]	39.14	0.2	0	9.8	0.2	0.2	1
20[a]	39.77	0.2	6.3	0.2	4.9	0.1	2.7
21[a]	41.73	0	0	1.1	0	0	0.6
22[a]	42.35	0	1.5	0	0.6	0.1	0
23[a]	42.36	0.1	0.7	0.1	0.8	0	0
24[a]	44.61	0.2	2.1	0	1.2	0.2	0.6
25[a]	44.98	0.2	0.4	1	0.4	0.1	0
26[a]	46	0	0.9	0	1	0.1	0.2
		90.4	84.5	85.6	87.2	92.5	72

[a]Local modes.

Table 6 Orthogonality of sine dwell modes[a]

Mode	201	101	501	404	301	601	2050	702	803	902	2902	1503	2002	1801
201	1	0.32	0.20	−.04	0	0.03	−0.02	−0.02	−0.01	0	0.01	−0.01	0.01	−0.01
101		1	0.10	.04	0.05	0.15	0.08	−0.01	−0.02	0	0	−0.01	0	0.01
501			1	−0.19	0.16	−0.17	−0.04	−0.01	0.01	0	−0.01	0.02	0.01	0
404				1	0.15	−0.20	−0.16	0.04	0.01	0.02	0	−0.02	−0.01	−0.03
301					1	−0.22	−0.13	0.02	0.04	−0.05	0.01	0.02	0.03	0.02
601						1	−0.26	−0.06	−0.08	0.08	0	−0.02	−0.02	−0.01
2050							1	0.80	0.01	−0.07	−0.01	−0.05	0	0.02
702								1	0.08	−0.19	−0.02	−0.01	−0.01	0
803									1	0.12	0	0.02	0.03	0.01
902										1	0	0	0.02	0.02
2902											1	−0.09	−0.05	−0.05
1503												1.00	0	−0.02
2002													1	0.20
1801														1

[a]Shaded numbers are local modes.

Table 7 Orthogonality of multishaker random modes[a]

Mode	1	2	3	4	5	6	7	8	9	10	11	12	13	14	15	16	17	18	19	20	21	22	23	24	25
1	1	0.02	−0.16	0.04	−0.03	−0.04	0.04	−0.04	−0.02	−0.01	0.02	0	−0.07	0.02	0	0.01	0.01	−0.01	−0.01	−0.02	−0.05	0	0.05	0.06	0.03
2		1	0.02	−0.04	0.04	−0.04	0	−0.02	−0.02	0	−0.01	0	−0.03	0.05	0	−0.01	−0.01	0.03	0.02	−0.01	0.02	0	−0.02	0.02	0
3			1	0.01	−0.03	−0.02	0.01	0.01	0	−0.01	−0.03	0.02	−0.07	−0.02	0.01	0.01	0.01	−0.01	−0.01	−0.22	0.05	−0.06	0.08	0.06	0.01
4				1	0.05	−0.04	0.01	−0.07	−0.02	−0.02	0.04	0.10	−0.06	0.15	0	−0.02	0.01	0.01	0.02	−0.06	0.02	0.01	−0.06	−0.01	−0.02
5					1	0.05	0.02	−0.01	−0.02	0.02	0.12	0.17	0	0.08	−0.02	−0.02	0.01	0.03	−0.01	−0.16	0.03	0.02	0.01	−0.05	−0.02
6						1	−0.03	−0.02	0.02	−0.07	0.04	0.06	0.07	0.02	0.09	0.09	−0.02	0.01	−0.03	−0.09	0.03	−0.03	0.07	−0.03	−0.03
7							1	0.07	−0.04	−0.14	−0.02	−0.04	0.04	−0.01	−0.04	−0.05	0	0	0.02	−0.03	−0.01	0	0.01	0.03	0.03
8								1	−0.04	0.25	−0.23	0	−0.02	0.01	0	−0.01	0.04	0	−0.01	0.01	0	0	0.02	0	0.01
9									1	0.03	−0.13	−0.10	−0.03	0.44	0.09	0.09	−0.07	−0.03	−0.05	−0.10	0	−0.01	0.05	0.08	0.01
10										1	0.33	−0.08	−0.36	−0.03	−0.04	0.01	−0.04	−0.01	−0.03	−0.06	−0.03	0	0.02	0.02	0.01
11											1	0.40	−0.25	0.07	−0.04	0.02	0	−0.03	−0.01	−0.07	0.01	−0.09	0.05	0	−0.04
12												1	0.05	0.05	0.03	0.03	0.03	0.01	−0.03	−0.09	0.08	0.19	0.09	−0.06	−0.10
13													1	−0.05	0	0.20	−0.02	0.07	−0.18	−0.03	0.14	−0.04	0.04	−0.14	−0.11
14														1	0.34	0.33	0.22	0.11	−0.10	−0.05	0.01	−0.01	0.10	0.05	−0.11
15															1	0.50	−0.09	0.01	−0.15	−0.13	0.18	−0.05	0.15	−0.19	−0.13
16																1	−0.06	0	−0.18	−0.14	0.14	0.01	0.12	−0.13	−0.11
17																	1	0	0.06	0.07	−0.04	−0.04	−0.02	0.03	−0.02
18																		1	−0.46	0.06	0.12	−0.1	0	−0.02	−0.02
19																			1	0.01	−0.08	−0.06	−0.14	−0.15	0.10
20																				1	−0.37	0.45	−0.34	0.29	0.07
21																					1	−0.59	−0.23	−0.54	−0.01
22																						1	−0.30	0.17	0.03
23																							1	−0.14	−0.07
24																								1	0.27
25																									1

[a]Shaded numbers are local modes.

Table 8 Cross orthogonality between sine dwell and multishaker random modes[a]

Mode	1	2	3	4	5	6	7	8	9	10	11	12	13	14	15	16	17	18	19	20	21	22	25
201	1	−0.02	−0.06	0.06	−0.04	0.01	0.02	−0.04	0.02	0	0.03	0.01	−0.07	0.05	0.01	0.01	0.03	0	−0.02	−0.06	−0.01	−0.03	0.07
101	0.39	1	−0.06	−0.26	0.13	0.01	−0.01	−0.03	−0.02	0	0	−0.01	−0.03	0.04	−0.01	−0.02	−0.01	0	−0.01	−0.04	0.02	−0.02	0.02
501	0.33	−0.08	−1	−0.35	0.10	0.08	−0.01	0	−0.02	0.06	0.07	−0.04	0.08	−0.03	0	0	−0.02	0	0.01	0.22	−0.05	0.07	−0.07
404	−0.12	−0.13	0.63	−1	0.25	0.01	−0.01	0.10	0.08	−0.01	−0.06	−0.01	0.03	−0.12	0	0.02	0.03	−0.02	−0.01	−0.13	0	−0.06	0.13
301	0	−0.03	0.09	0.08	1	0.06	0.01	−0.01	−0.02	0.02	0.07	0.08	0.01	0.07	0	−0.01	0.02	0.03	−0.01	−0.14	0.01	0.05	−0.01
601	0.09	0.27	0.10	0.22	−0.22	−1	0.31	0.09	−0.10	−0.04	−0.07	0.02	−0.04	−0.06	−0.09	−0.10	−0.03	−0.02	0.02	0.02	0.05	−0.03	−0.06
2050	−0.06	0.25	0.03	0.18	−0.22	1	0.87	0.84	−0.18	0.57	0.10	−0.06	−0.20	−0.07	−0.10	−0.07	−0.01	−0.10	0.06	−0.11	−0.03	0	0.03
702	−0.05	0	0.04	−0.04	0.04	0.24	0.53	1	−0.10	0.70	0.27	−0.05	−0.31	0.02	−0.11	−0.10	0.03	0	0.02	−0.06	−0.06	0	0.02
803	−0.05	−0.04	−0.04	0	0.06	0.06	−0.03	0.12	1	0.15	−0.12	−0.09	−0.04	0.35	0.05	0.07	−0.29	0.01	−0.08	−0.13	0.01	−0.02	0.05
902	0.01	−0.03	−0.05	−0.06	−0.08	0.01	0.03	0.43	0.13	−0.62	−1	0.03	0.42	−0.07	0.11	0.08	0	−0.02	0.06	0.03	0.03	−0.01	0
2902	0.07	0.02	0.04	0.05	0.11	0.06	−0.05	−0.06	0.02	0	0.25	0.34	−0.38	−0.30	0.99	−0.65	−0.23	−0.24	1	−0.11	−0.03	−0.72	0.27
1503	−0.02	−0.03	−0.03	0	0.02	0.02	0.01	−0.01	−0.02	−0.03	−0.04	0.01	0.09	0.09	−0.02	−0.02	−0.01	1	−0.45	0.05	0.12	−0.02	−0.01
2002	0.06	0.01	0.01	0.03	0.03	0	−0.01	−0.05	0.07	0.03	−0.03	−0.11	0.02	0.08	0.11	0.12	−0.12	0.03	1	0.33	−0.98	0.68	0.18
1801	−0.01	0.06	0.03	0.09	0.02	−0.02	−0.02	0	0.03	0	−0.05	0.06	0.23	0.25	−0.04	0	0.03	−0.04	0.36	0.65	−0.47	0.71	1

[a]Shaded numbers indicate questionable coupling.

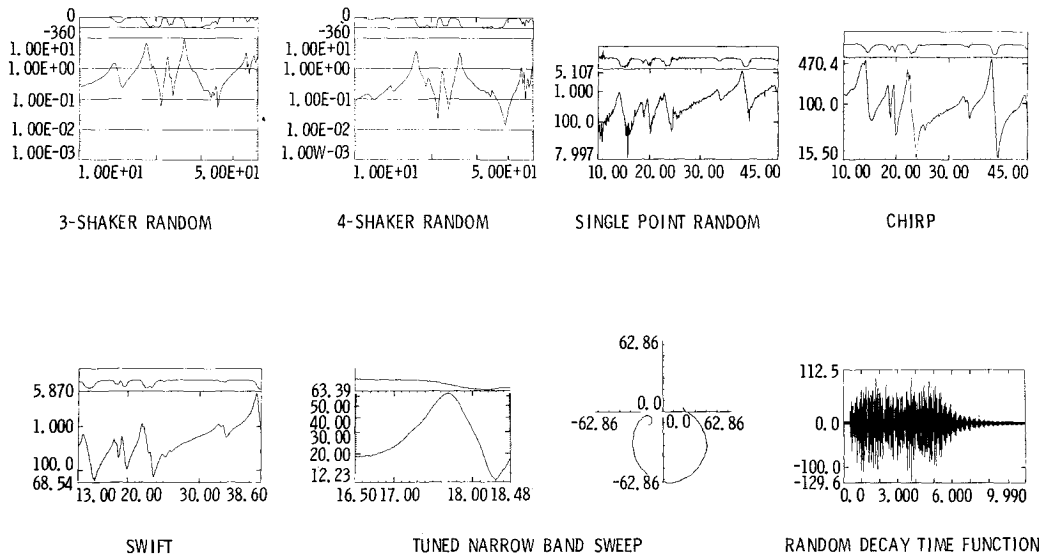

Fig. 2 Response functions of modal test.

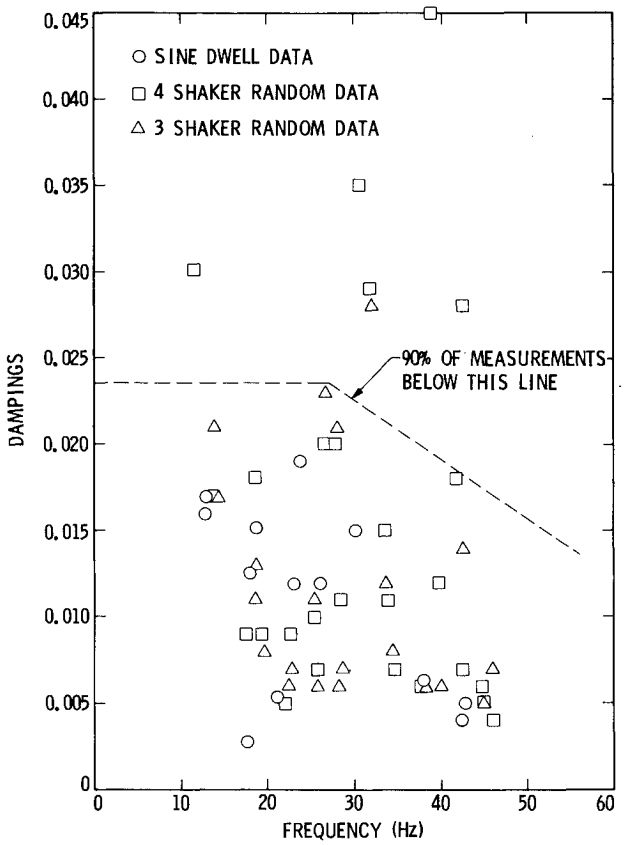

Fig. 3 Modal dampings.

Table 9 Mode shape comparison

Component	TAM 1 (11.08 Hz)		SD 201 (12.70 Hz)		MSR 1 (11.46 Hz)	
SXA tip in *Y*	1	(1)	1	(1)	1	(1)
SXA base ring in *Y*	0.49	(2)	0.47	(2)	0.49	(2)
SXA C.G. in *Y*	0.25	(3)	0.30	(3)	0.30	(3)
SXA tip in *X*	0.10	(4)	−0.22	(4)	−0.27	(4)
EDP in *Z*	0.08	(5)	0.06	(7)	0.06	(7)
Mag. canister in *Z*	0.08	(6)	0.05	(8)	0.06	(9)
Science boom hinge in *Z*	0.08	(7)	0.07	(6)	0.09	(6)
PLS in *Z*	0.08	(8)	0.04		0.03	
Mag. canister in *Z*	0.07	(9)	0.05	(9)	0.05	(10)
Mag. canister I/F in *Z*	0.07	(10)	0.05		0.05	
RSS 1			0.330		0.384	
RSS 2					0.059	

Table 10 Mode shape comparison

Component	TAM 6 (20.04 Hz)		SD 601 (21.67 Hz)		MSR 6 (22.06 Hz)	
+ *X* RTG in *Z*	1	(1)	0.69	(4)	0.35	(5)
− *X* RTG in *Z*	−0.97	(2)	−0.94	(2)	−1	(1)
RRH in *Y*	−0.32	(3)	−0.66	(5)	−0.65	(2)
SXA tip in *X*	−0.26	(4)	−0.11		0.15	
Mag. canister in *X*	0.23	(5)	−0.37		0.26	(7)
Mag. canister I/F in *X*	0.20	(6)	1	(1)	0.28	(6)
EPD in *X*	0.17	(7)	0.66	(6)	0.21	
− X Thruster in *Z*	0.16	(8)	−0.21		0.17	
BUS in *X*	−0.16	(9)	−0.56	(9)	−0.16	
BUS in *X*	−0.16	(10)	0.62	(7)	−0.18	
RSS 1			1.66		0.84	
RSS 2					1.59	

objectives for doing modal testing on a variety of systems and each has its own particular requirements and constraints. These individual conditions may ultimately determine the selection of testing method. Nevertheless, based on the present experiences, the evaluations are as follows:

1) All methods are able to extract the major modes of importance.

2) The modal parameters obtained by different methods are generally consistent.

3) Frequency response function methods extract more modes than the multishaker sine dwell method.

4) When compared to the frequency response function methods, the sine dwell method is able to make a larger amplitude response to investigate nonlinear effects during modal testing.

5) The sine dwell test provides a unique opportunity for the test engineer to interact with the test specimen on a mode-by-mode basis. The structure can be explored with eyes, ears, and hands during the test. This "hands-on-the-structure" approach is key to gaining personal insight into the structure's behavior.

6) Actual testing time for the frequency response function methods is only a small fraction of that of the sine dwell method.

7) Data processing for the frequency response function methods can be made in almost real time. The data from multishaker random tests were processed immediately by a VAX 11/780 computer and identified modal parameters were available within twenty-four hours.

8) Multishaker random tests are simplified by not repeating the test for other shaker configurations as is required by the single-shaker tests.

9) Input energy distribution among modes is more even for the multishaker random test than the single-shaker tests.

10) The operational simplicity of the single-shaker tests is quite remarkable. This is definitely an advantage for those who lack extensive modal testing experience.

11) For the SWIFT method, the frequency response functions are obtained by exciting the test specimen sinusoidally at discrete frequency for a finite period before moving on to

Table 11 Kinetic energy distribution

Component	TAM 1 (11.08 Hz)			SD 201 (12.70 Hz)			MSR 1 (11.46 Hz)		
	X	*Y*	*Z*	*X*	*Y*	*Z*	*X*	*Y*	*Z*
SXA TIP	0.7	73.5	0	3.5	75.2	0	5.5	76.5	0.3
BUS	0	1.6	0.2	0	0.9	0.2	0.2	0.1	0
BUS	0	2.5	0.3	0.1	1.2	0.4	0.1	0.2	0.1
Oxidizer 2	0	1.8	0.3	0	1.3	0.1	0.1	0.4	0
Oxidizer 1	0	1.8	0.3	0.1	1.0	0.1	0.4	0.6	0
Sum	0.9	93.9	4.7	4.1	92.9	2.8	7.0	90.5	2.1

Table 12 Kinetic energy distribution

Component	TAM 6 (20.04 Hz)			SD 601 (21.67 Hz)			MSR 6 (22.06 Hz)		
	X	*Y*	*Z*	*X*	*Y*	*Z*	*X*	*Y*	*Z*
Oxidizer 2	4.2	0.1	0	7.3	0.2	0.1	4.3	0.7	0.1
Fuel 2	1.5	0.2	0	4.1	0.8	0	2.0	0.3	0
Oxidizer 1	4.9	0	0	13.7	0.8	0	7.7	0.2	0.1
Fuel 1	2.2	0.1	0	5.0	0.6	0	4.4	0.4	0.1
+ *X* RTG	0	0	39.2	0.2	0	7.8	0	0	6.2
− *X* RTG	0	0	36.7	0.4	0	14.5	0	0	50.5
Sum	19.5	1.3	77.9	65.5	6.2	25.7	30.8	8.1	59.6

another frequency with incremental value. This method seems to perform better among the single-shaker tests by having cleaner frequency response functions.

12) Damping data from the curve-fitting results of the frequency response function tests are very inconsistent compared with those from the sine dwell tests. This is the case in the present study as well as in previous ones (Refs. 3 and 4). Perhaps this is contributed to the fact that the responses due to random excitation are not sensitive with respect to dampings.

Concluding Remarks

In addition to the evaluation of various modal testing methods, the objective of the present study also includes the attempts to rank these methods according to their capabilities. However, it has failed because each method has its own unique merit. Also, the fact that the "correct" modal parameters are not known a priori makes it hard to establish the relative accuracy of each method. However, it should be listed that the sine dwell method provided the most consistent correlation with respect to the overall comparison. The selection of the proper modal testing method should be determined by its requirements and constraints, and by the nature of the test article. It should be reassuring that the age-old sine dwell method still possesses certain capabilities that other modern frequency response methods cannot provide. Perhaps this is the reason why this method, which was developed in the 1950s, is still popular among the aerospace industry. On the other hand, the modern modal test methods that use data processing demonstrate their powerful capabilities and tremendous operational ease. It is this author's belief that these frequency response function methods must mature further to become the standard practice.

Acknowledgments

This research was carried out by the Jet Propulsion Laboratory, California Institute of Technology, under Contract NAS7-918. This task was sponsored by Samuel L. Venneri, NASA Office of Aeronautics and Space Technology, Code RM.

References

[1]Lewis, R.C. and Wrisley, D.L., "A System for the Excitation of Pure Natural Modes of Complex Structure," *Journal of the Aeronautical Sciences*, Vol. 17, No. 11, 1950, pp. 705–722.

[2]Klosterman, A. and Zimmerman, R., "Modal Survey Activity via Frequency Response Function," SAE Paper 751063, 1975.

[3]Leppert, E.L., Lee, S.H., Day, F.D., Chapman, C.P., and Wada, B.K., "Comparison of Modal Test Results: Multi-Point Sine Versus Single Point Random," SAE Paper 760879, 1976.

[4]Hanks, B., Ibrahim, S.R., Miserentino, R., Lee, S.H., and Wada, B.K., "Comparison of Modal Test Method on the Voyager Payload," SAE Paper 781044, 1978.

[5]Allemang, R.J., "Experimental Modal Analysis," *Modal Testing and Model Refinement*, Volume ADM-Vol. 59, ASME, NY, 1983, pp. 1–29.

[6]Caughey, T.K. and O'Kelly, M.E.J., "Classical Normal Modes in Damped Linear Dynamics Systems," *Journal of Applied Mechanics*, Vol. 32, Vol. 87, Series E, 1965, pp. 583–588.

[7]Asher, G.W., "A Method of Normal Mode Excitation Utilizing Admittance Measurement," *Proceedings of the National Specialists' Meeting, Institute of Aeronautical Science: Dynamics and Aeroelasticity*, Nov. 1958, pp. 69-76.

[8]Ibanez, P., "Force Appropriation by Extended Asher's Method," SAE Paper 760873, 1976.

[9]Morosow, G. and Ayre, R.S., "Force Apportioning for Modal Vibration Testing Using Incomplete Excitation," *Shock and Vibration Bulletin*, Vol. 48, Part 1, 1978, pp. 39–48.

[10]Anderson, J.E., "Another Look at Sine-Dwell Mode Testing," *Journal of Guidance and Control*, Vol. 5, July–Aug. 1982, p. 358.

[11]Vold, H., Kundrat, J., Rocklin, G., and Russell, R., "A Multi-Input Modal Estimation Algorithm for Mini-Computers," SAE Paper 820194, 1982.

[12]Brigham, E.O., *The Fast Fourier Transform*, Prentice-Hall, Englewood Cliffs, NJ, 1974.

[13]Chen, J.C. and Trubert, M., "Galileo Model Test and Pretest Analysis," *Proceedings of the 2nd International Modal Analysis Conference*, Union College, Schenectady, NY, 1984, pp. 796–802.

[14]Guyan, R.J., "Reduction of Mass and Stiffness Matrices," *AIAA Journal*, Vol. 3, Feb. 1965, p. 380.

[15]Trubert, M., "Assessment of Galileo Modal Test Results for Mathematical Model Verification," AIAA Paper 84-1066, May 1984.

[16]Stroud, R.C., Pamidi, M.R., and Bausch, H.P., "Some Measurement and Analysis Methods Used in the Galileo Spacecraft Modal Survey," AIAA Paper 84-1067, May 1984.

[17]Chen, J.C. and Hunt, D.L., "Application of Multiple Input Random and Polyreference Analysis Techniques to the Galileo Spacecraft Modal Tests," AIAA Paper 84-1069, May 1984.

[18]Pappa, R.S., "Galileo Spacecraft Modal Identification Using Eigensystem Realization Algorithm Test," AIAA Paper 84-1070, May 1984.

[19]Coppolino, R.N., "A Simultaneous Frequency Domain Technique for Estimation of Modal Parameters from Measured Data," SAE Paper 811046, Oct. 1981.